Bull. Mater. Sci., Vol. 33, No. 1, February 2010, pp. 33–41. © Indian Academy of Sciences.

Effects of SiO_2 and TiO_2 fillers on thermal and dielectric properties of eco-friendly bismuth glass microcomposites of plasma display panels

SHIV PRAKASH SINGH, KARAN PAL, ANAL TARAFDER, MOUSUMI DAS, KALYANDURG ANNAPURNA and BASUDEB KARMAKAR*

Glass Division, Central Glass and Ceramic Research Institute (Council of Scientific and Industrial Research), Kolkata 700 032, India

MS received 12 November 2008; revised 18 March 2009

Abstract. **The effects of SiO_2 (amorphous) and TiO_2 (crystalline, rutile) fillers on softening point (T_s), glass transition temperature (T_g), coefficient of thermal expansion (CTE), and dielectric constant (ε) of zinc bismuth borate, $ZnO–Bi_2O_3–B_2O_3$ (ZBIB) glass microcomposites have been investigated with a view to its use as the white back (rear glass dielectric layer) of plasma display panels (PDPs). The experimentally measured properties have also been compared with those of theoretically predicted values. Both the experimental and theoretical trends of these properties with added filler contents correlate very well. The interaction of fillers with glass which occurred during sintering at 560°C has also been monitored by XRD and FTIR spectroscopic analyses. The microstructures and distribution of fillers in the glass matrix have been analyzed by SEM images. It is observed that the fillers have partially dissolved in the glass at the firing temperature leaving some unreacted filler as residue which results in ceramic–glass microcomposites. In consideration of the desired properties of white back of PDPs, the addition of TiO_2 filler to ZBIB glass is found to be more preferable than SiO_2 filler. The addition of 10 wt% TiO_2 filler yielded T_s, T_g, CTE and ε values of 560°C, 480°C, 82×10^{-7}/K and 14·6 which are found to meet the desired values of <580°C, <500°C, $<83 \times 10^{-7}$/K and <15, respectively with respect to use of PD200 glass as substrate in PDP technology.**

Keywords. **Composite materials; FTIR; thermal properties; dielectric properties.**

1. Introduction

At present, the plasma display panel (PDP) is competing with the liquid crystal display (LCD) in wall-hung television (TV) applications (Shinoda *et al* 2000) and its popularity is increasing very rapidly. The PDP has several advantages compared to LCD such as high dimension TVs (about 102 inches), wide viewing angle (160°), best bright room contrast ratio, excellent colour fidelity, least motion artifact and very gentle to eyes. PDP requires several glass powders of some specified thermal and dielectric properties for its construction such as white back (rear glass dielectric layer), barrier rib (partition between phosphor cavities), etc. In PDP white dielectric (white back—the rear glass dielectric) is used as the insulating film of the address electrodes on the rear glass substrate and give support to barrier rib. Glass powders are widely used as white back materials with addition of various types of ceramic oxide (e.g. SiO_2, TiO_2, etc) as filler for adjustment of its desired properties as well as improvement of its mechanical strength. Lead (Pb) based frits of $PbO–B_2O_3–ZnO$ and $PbO–B_2O_3–SiO_2$ glasses are very popular as the commercial materials for PDP (Shiro *et al* 1998; Hiromitsu *et al* 2000; Hwang *et al* 2002). Lead is used in the glass due to its low softening point (T_s), high refractive index as well as adjustable properties required for PDP (Masahi and Shinji 1999; Naoya and Kazuhiro 1999; Kim and Sannoo 2002). Here, lead oxide (PbO) is used to the extent of 60–80 wt.%, which creates problem due to its deleterious effect to both health and the environment (Chang *et al* 2001). So recently some Pb-free glasses such as $BaO–ZnO–B_2O_3$ (Kim *et al* 2005), $Bi_2O_3–B_2O_3–BaO–ZnO$ (Song and Choi 2006; Song *et al* 2006), $BaO–B_2O_3–SiO_2$ (Lim *et al* 2006) etc have been reported as alternate materials for use in PDP technology. The effects of various types of crystalline fillers (e.g. SiO_2, TiO_2, Al_2O_3, ZrO_2, MgO, etc) in some lead-free glasses for PDP application are reported (Kim *et al* 2005, 2006; Lim *et al* 2006; Shin *et al* 2006a, b). But only a very few glass compositions have been reported for white back application. To the best of our knowledge, there is no report on the effect of SiO_2 and TiO_2 fillers on the properties of $ZnO–Bi_2O_3–B_2O_3$ (ZBIB) glass for use as white back of PDP.

In this study, bismuth oxide based glass has been selected as a substitute of lead oxide based glasses as it is next to lead in the periodic table which has low melting tem-

*Author for correspondence (basudebk@cgcri.res.in)

perature (820°C) and high refractive index (n = 2·5) as lead oxide (m.p. = 880°C, n = 2·24). For selection of white back glass composition for PDP, it is important to achieve at least three decisive properties such as softening point (T_s), coefficient of thermal expansion (CTE) and dielectric constant (ε). It is observed that there are a very few reports on microcomposites for PDP application which have addressed all these three decisive properties simultaneously (Lim *et al* 2006). SiO_2 (CTE = 5·5 × 10^{-7}/K, ε = 3·8 at 1 MHz frequency) and TiO_2 (CTE = 80–100 × 10^{-7}/K, ε = 80–100 at 1 MHz frequency) having just opposite values (low and high, respectively) of CTE and dielectric constant have been selected as fillers in this investigation.

In view of above, in this paper we report the effects of SiO_2 (amorphous) and TiO_2 (rutile) fillers on the softening point (T_s), glass transition temperature (T_g), coefficient of thermal expansion(CTE) and dielectric constant (ε) of the microcomposites derived from the (wt.%) 19ZnO–46Bi_2O_3–35B_2O_3 (ZBIB) glass. The interaction between the fillers and the glass which occurred during sintering is also examined by XRD, FTIR and SEM micrographic analyses.

2. Experimental

2.1 *Preparation of glass and microcomposite*

The chemical composition (wt.%) of glass was 19ZnO–46Bi_2O_3–35B_2O_3 (ZBIB). The batch was prepared using the high purity raw materials such as ZnO (GR, 99%), Bi_2O_3 (99%) and H_3BO_3 (GR, 99·5%) of Loba Chemie. About 600 g glass was melted using these raw materials in a platinum crucible in an electrically heated raising hearth furnace at 1150°C for 2 h in air with intermittent stirring. The molten glass was quenched by casting into an iron plate. The quenched glass was initially crushed in a stainless steel mortar and then pulverized in a planetary ball mill (Retzch, Model PM100) using zirconia jar and ball to obtain final glass powders of 14·4 μm size (d_{50}).

Table 1. Composition of microcomposites derived from glass.

Sample identity	Composition (wt.%)		
	Glass (ZBIB)	Added SiO_2 filler	Added TiO_2 filler
G[a]	100		
GS5	95	5	
GS10	90	10	
GS15	85	15	
GS20	80	20	
GT5	95		5
GT10	90		10
GT15	85		15
GT20	80		20

[a]Composition (wt.%) of glass (G): 19ZnO–46Bi_2O_3–35B_2O_3 (ZBIB).

The pulverized ZBIB glass powders were mixed in isopropanol medium with appropriate amounts of microsilica, SiO_2 (Pooja Enterprises, 99·5%, d_{50} = 1·5 μm) and titania, TiO_2 (Aldrich, 99·9%, d_{50} = 3·2 μm) fillers in an agate mortar. All the powders were then granulated using 2 wt% aqueous solution of polyvinyl alcohol (PVA) followed by pressing uniaxially into disk or cylindrical shape under a pressure of 500 kgf/cm^2 and then dried. It was sintered at 560°C for 2 h in air for measurement of coefficient of thermal expansion, dielectric constant, XRD and FTIR spectra. The composition of composites are enlisted in table 1.

2.2 *Characterization technique*

The softening point (T_s) of the dried disk was measured by a glass softening point system (Harrop/Labino, Model SP-3A) with an accuracy of ±1°C. The instrument was previously calibrated with a NBS (National Bureau of Standards, USA) standard glass of known softening point. The CTE and T_g of the sintered microcomposite cylinders were measured with an accuracy of ±0·2% using a horizontal-loading dilatometer (Netzsch, Model 402C) after calibration with standard alumina supplied with the instrument by the manufacturer. The CTE in the temperature range 50–350°C was reported here. The dielectric constant was measured with an accuracy of ±0·5% at a frequency of 1 MHz using a LCR meter (Hioki, Model 3532-50 LCR Hitester) at 25°C. The instrument was calibrated previously by Suprasil-W silica glass (ε = 3·8). XRD data of powder samples were recorded using XPERTPRO diffractometer with 2θ varying from 10° to 80° using Ni filtered CuKα (λ = 1·5406 Å) at 25°C, generator power of 45 kV and 35 mA. FTIR spectra were recorded by dispersing the sintered glass and composite powders in KBr with a Perkin-Elmer FTIR spectrometer (Model 1615) at a resolution of ±2 cm^{-1} after 16 scans. It was calibrated with a polystyrene film supplied by the instrument manufacturer. The SEM images of the samples were carried out in LEO S430i instrument at 15 kV. The samples were examined after Au coating on the surface to pass the electron beam through it.

Glass properties such as Littleton softening point (T_{Lt}), CTE, and T_g were theoretically calculated (predicted) using SciGlass (Glass Properties Information System, Version 6.7) software following the Priven-2000 method (Priven 1998, 2004; Priven and Mazunin 2003; SciGlass Version 6.7) and dielectric constant by the method of Kharjuzov and Zorin (SciGlass Version 6.7).

3. Results and discussion

3.1 *Particle size distribution*

The extent of interaction of glass and fillers at the sintering temperature is largely dependent on their particle size

and its distribution. Thus, the particle size distribution of ZBIB glass powder, TiO_2 and SiO_2 fillers are shown in figure 1. It is seen that all the powders exhibit a bimodal particle size distribution. The median particle sizes (d_{50}) of ZBIB glass powder, TiO_2 and SiO_2 fillers are found to be 14·4, 3·2 and 1·5 μm, respectively.

3.2 *XRD analysis*

As the reaction of fillers (SiO_2 and TiO_2) with glass during firing at 560°C is fundamental to the formation of filler–glass microcomposites, thus, they have been examined by XRD analysis. The variation of XRD pattern of microcomposites with added TiO_2 filler content is shown in figure 2. ZBIB glass is X-ray amorphous (figure 2, curve a). Since the added SiO_2 filler is amorphous, so all the SiO_2 containing microcomposites are found to be X-ray amorphous and do not exhibit any characteristic XRD peak (not shown here). On the other hand, TiO_2 filler is crystalline, rutile (see figure 2, curve f), so the TiO_2 containing microcomposites exhibit gradual development of XRD pattern of rutile TiO_2 (JCPDS card No.: 21-1276) with suppressed amorphous character of the resultant composites. XRD patterns clearly depict that the filler has partially dissolved in glass during sintering leaving behind some residual filler in the glass matrix. This observation correlates well with those of FTIR spectral study as discussed later (see § 3.3). Thus, it is clear from XRD analysis that SiO_2 (amorphous) and TiO_2 (crystalline) filler containing microcomposites are of amorphous-in-amorphous and crystal (ceramic)-in-amorphous characteristics, respectively.

3.3 *FTIR spectral analysis*

The FTIR spectra of SiO_2 and TiO_2 containing microcomposites are depicted in figures 3 and 4, respectively.

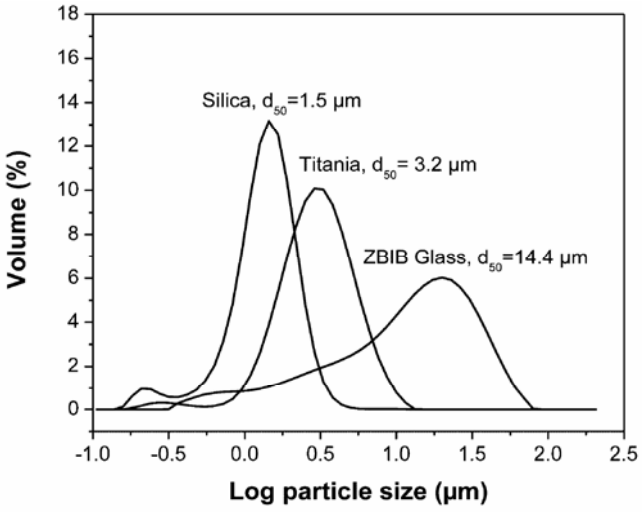

Figure 1. Particle size distribution of ZBIB glass, filler SiO_2 and TiO_2 powders.

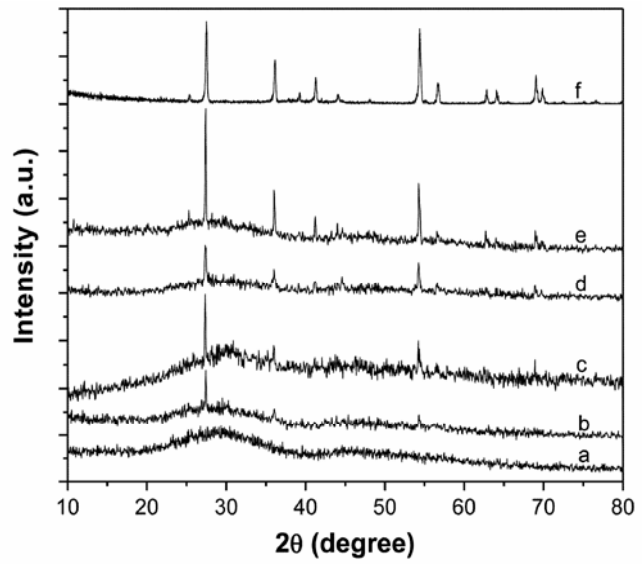

Figure 2. Variation of XRD patterns with added TiO_2 filler content: (a) glass, G, (b) GT5, (c) GT10, (d) GT15 and (e) GT20 (for composition, see table 1). XRD pattern (f) of added TiO_2 filler is also shown for comparison.

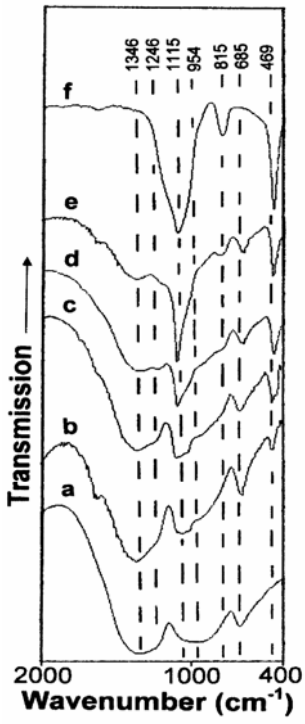

Figure 3. FTIR spectra of glass and composites: (a) glass, G, (b) GS5, (c) GS10, (d) GS15, (e) GS20 (for composition, see table 1). FTIR spectra (f) of added SiO_2 filler is also shown for comparison.

Table 2. IR band position and its assignment in glass, composites and SiO_2 filler.

Sample identity/band position (cm^{-1})						
G	GS5	GS10	GS15	GS20	SiO_2 filler	Band assignment
1346 (s, b)	1346 (s, b)	1346 (s, b)	1346 (m, b)	1346 (m, b)		B–O–B (as-s)
	1246 (w)	1246 (w)	1213 (m)	1215 (m, b)		B–O–Si (as-s)
	1069 (b)	1023 (b)	1108 (m)	1115 (s)	1115 (v, s)	Si–O–Si (as-s), B–O–Si (as-s)
954 (b)	946 (b)	946 (b)	946 (w)	939 (sh)		B–O–B (s-v), B–O–Si (as-s)
			815 (w)	815 (m)	815 (s)	O–Si–O (s-s)
685 (s)	685 (s)	685 (s)	669 (s)	669 (s)		Bi–O–Bi (s-v)
	469 (m)	469 (s)	469 (s)	469 (s)	469 (v, s)	Si–O–Si (b-v)

s = strong, b = broad, m = medium, w = weak, sh = shoulder, v = very, as-s = asymmetric stretching vibration, s-s = symmetric stretching vibration, s-v = stretching vibration, b-v = bending vibration.

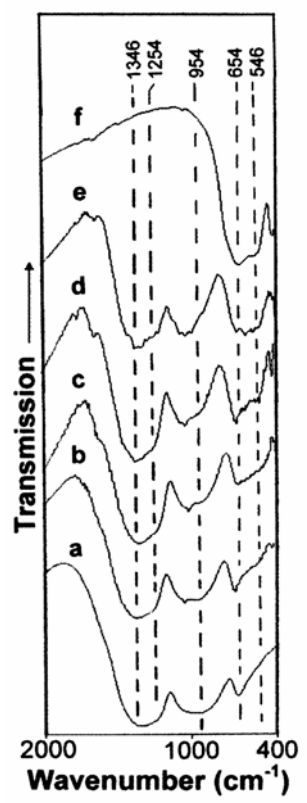

Figure 4. FTIR spectra of glass and composites: (a) glass, G, (b) GT5, (c) GT10, (d) GT15, (e) GT20 (for composition, see table 1). FTIR spectra (f) of added TiO_2 filler is also shown for comparison.

Their IR band positions along with assignments are also provided in tables 2 and 3, respectively. The ZBIB glass exhibits three distinct bands around 1346, 954 and 685 cm^{-1}, which are attributed to asymmetric stretching vibration of B–O–B bond of the trigonal [BO_3] units, stretching vibration of B–O–B bond of the tetragonal [BO_4] units, and bending vibration of B–O–B linkages, respectively of the borate glass networks (Kamitsos *et al* 1987; Fuxi 1992; Motke *et al* 2002). The band at 685 cm^{-1} is also due to the stretching vibration of Bi–O–Bi bond of [BiO_6] octahedral units (Kharlamov *et al* 1996; Baia *et al* 2003). The SiO_2 filler also exhibits three intense bands at around 1115, 815 and 469 cm^{-1} which are attributed to asymmetric stretching vibration of Si–O–Si bond, symmetric stretching vibration of O–Si–O bond and bending vibration of Si–O–Si bond of [SiO_4] tetrahedral unit, respectively (Fuxi 1992). It is seen from figure 3 that with increasing SiO_2 filler in the composites, GS5 to GS20, all these three bands in microcomposites gradually become more intense along with the intensity decrease and changes of shapes of all the three bands of the ZBIB glass. These observations have been more clearly enlisted in table 2. The bands at around 1246, 1069 and 946 cm^{-1} are attributed to asymmetric vibration of B–O–Si bond (Fuxi 1992). The band at around 669 cm^{-1} is assigned to Bi–O–Si asymmetric stretching vibration (Fuxi 1992). This fact clearly indicates the distinct interaction of ZBIB glass with SiO_2 filler at the sintering temperature and formation of bonds with SiO_2.

The TiO_2 filler exhibits one very strong and doublet absorption band peaking at 654 and 546 cm^{-1} which are due to stretching vibrations of Ti–O–Ti bond of [TiO_6] octahedra (Last 1957; Rao 1963). It is seen from figure 4 that with increasing TiO_2 filler content in the composites GT5 to GT20, the band at 685 cm^{-1} of the ZBIB glass gradually undergoes pronounced change and the bands of TiO_2 filler at 654 and 546 cm^{-1} gradually become more intense. It indicates the formation of Ti–O–Bi bonds. In addition, the 1346 and 954 cm^{-1} bands undergo changes with formation of medium intense band at around 1254, 1203, 1023 and 908 cm^{-1} which are due to asymmetric vibration of B–O–Ti bond (Uma and Nogami 2007). This is clearly shown in table 3. All these facts clearly indicate the distinct interaction of ZBIB glass with TiO_2 filler. It is seen from figures 3 and 4 that the nature of the spectra of microcomposites, in both SiO_2 and TiO_2 additions, gradually become closer to those of fillers. This indicates that the fillers have partially dissolved in the glass leaving behind residual fillers in resultant microcomposites.

Table 3. IR band position and assignment in glass, composites and TiO_2 filler.

Sample identity/band position (cm^{-1})						
G	GT5	GT10	GT15	GT20	TiO_2 filler	Band assignment
1346 (s, b)	1346 (s, b)	1346 (s, b)	1346 (s, b)	1346 (s, b)		B–O–B (as-s)
	1023 (m)	1254 (w), 1023 (m)	1254 (w), 1023 (s)	1254 (w), 1023 (s)		B–O–Ti (as-s)
954 (s, b)	908 (m)	923 (m)	923 (w)	900 (sh)		B–O–B (as-s), B–O–Ti (as-s)
685	669 (s)	669 (s)	669 (s)	669 (s)		Bi–O–Bi (s-v), Ti–O–Bi (s-v)
	531 (sh)	531 (b)	539 (m)	539 (s)	654 (vs), 546 (vs)	Ti–O–Ti (s-v)

s = strong, b = broad, m = medium, w = weak, sh = shoulder, v = very, as-s = asymmetric stretching vibration, s-v = stretching vibration.

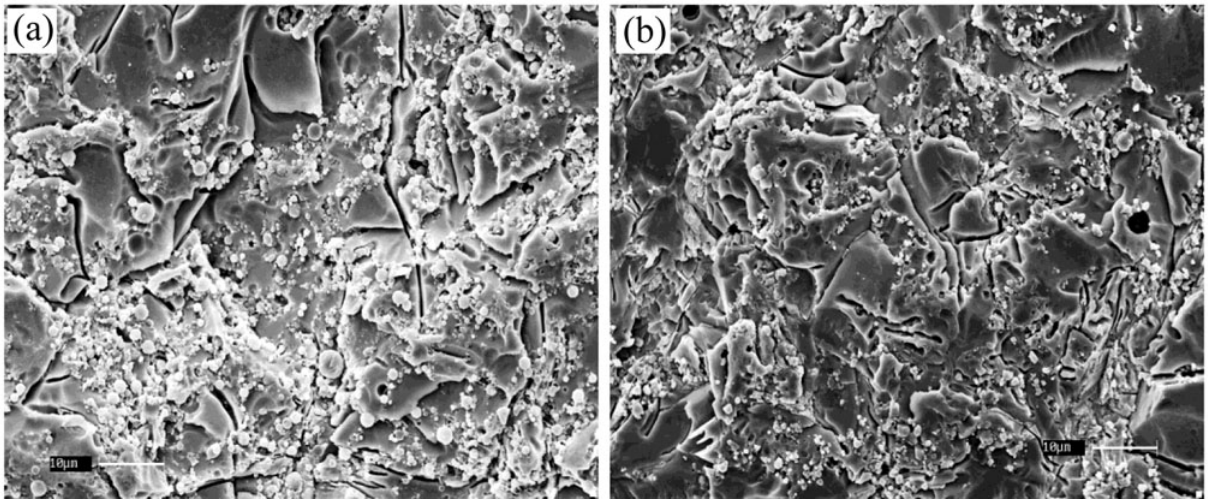

Figure 5. SEM micrographs of microcomposites (**a**) GS15 and (**b**) GT15 showing the distribution of SiO_2 and TiO_2 fillers, respectively in the glass matrix.

This is analogous to the observation of XRD analysis (see § 3.2).

3.4 *SEM micrograph analysis*

The microstructure of the sintered composites at 560°C with SiO_2 and TiO_2 fillers was characterized by SEM micrographs. Figure 5 depicts the morphology and distribution of residual SiO_2 and TiO_2 fillers in the glass matrix. The sintering of glass frits at such a low temperature means that the glass frits are softened enough to attack crystalline phases of the fillers, which yields uneven-shaped and increased fluidity for the realignment of the fillers. Some pores are found in the SEM micrographs which indicate that the density of the sintered microcomposites would be less than that of glass. SEM micrographs exhibit cracking of resulting microcomposites and its extent is more in SiO_2 containing sample (GS15) compared to that in TiO_2 containing sample (GT15). This is due to CTE mismatching between that of guest filler (SiO_2, low expansion) and host glass matrix (high expansion).

3.5 *Softening point and glass transition temperature*

The softening point (T_s) and glass transition temperatures (T_g) are gradually going up as the SiO_2 and TiO_2 filler contents increase from 5–20 wt%. A similar trend is observed in the theoretically predicted Littleton softening point ($T_{Lt.}$) and glass transition temperature as well. However, the experimental values in both the cases are lower than those of theoretical predictions. These facts are depicted in figures 6 and 7. The close correlation between the experimentally and theoretically calculated softening point and glass transition temperature trends clearly indicates that these properties are additive in nature with respect to the constituting chemical components. This is because of the fact that theoretical calculations of the T_{Lt}

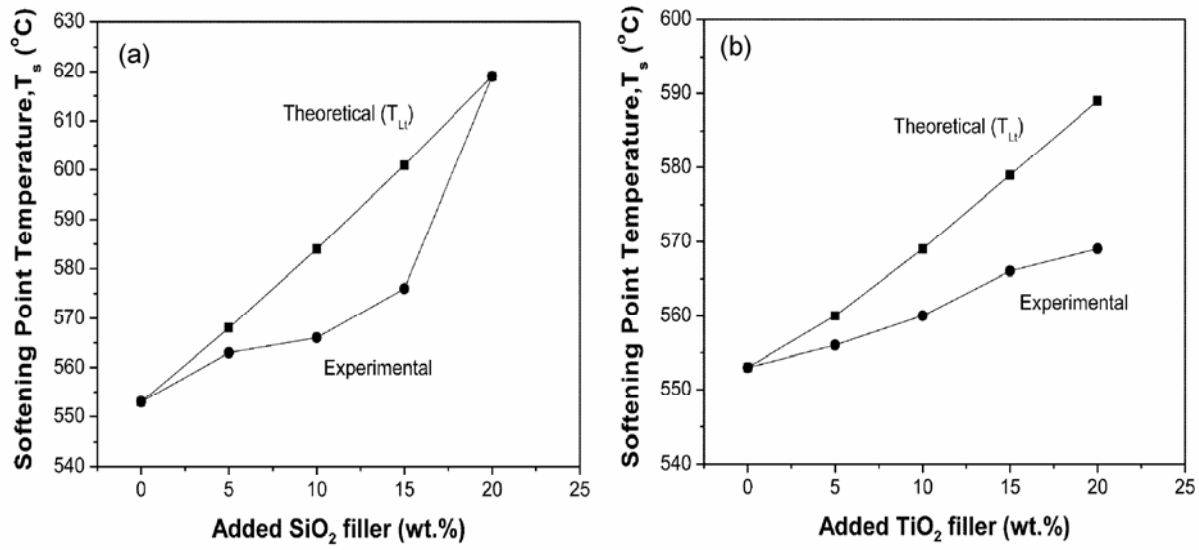

Figure 6. Comparison of variation of experimentally and theoretically predicted softening point temperature (T_s) as a function of added (**a**) SiO_2 and (**b**) TiO_2 fillers (for composition, see table 1).

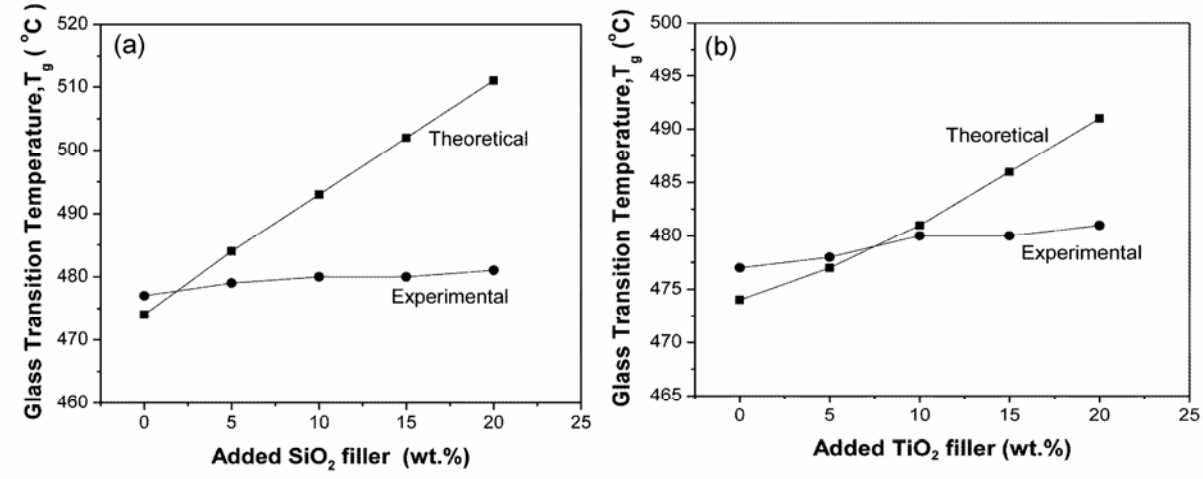

Figure 7. Comparison of variation of experimentally and theoretically predicted glass transition temperature (T_g) as a function of added (**a**) SiO_2 and (**b**) TiO_2 fillers (for composition, see table 1).

and T_g are based on additive mathematical formula (Priven 1998, 2004; Priven and Mazunin 2003) as shown below.

$$P = \sum_{i=1}^{N} g_{i,p} m_i n_i \sum_{i=1}^{N} m_i n_i, \quad (1)$$

where P is the property being calculated, i the index of the oxide; N the number of types of oxides forming the glass in question; m_i a molar fraction of the ith oxide; n_i is the number of atoms in the formula of the ith oxide and $g_{i,p}$ is a partial coefficient for the ith oxide.

A similar increasing trend of glass transition temperature with increasing SiO_2 content has been demonstrated by Vernacotola and Shelby (Vernacotola and Shelby 1993; Vernacotola 1994) for potassium niobium silicate glasses. Some properties of added SiO_2 and TiO_2 fillers are provided in table 4. It is seen that SiO_2 and TiO_2 have high melting points. The increase of T_s and T_g of micro-composites is due to high melting points of SiO_2 (1723°C) and TiO_2 (1850°C) fillers. It is also seen from figure 5 that SiO_2 filler has greater effect on softening point as compared to TiO_2 filler. This is due to higher Si–O bond strength (2·48) and Si field strength (1·54)

Table 4. Some properties of added SiO_2 and TiO_2 fillers.

Filler	Crystallinity	Melting point (°C)	CTE ($\times 10^{-7}$/K)	Dielectric constant (ε)	Si or Ti field strength (Z/a^2*)	Si–O or Ti–O bond strength (Z/a*)	Polariz-ability, α	Refractive index (n)
SiO_2	Amorphous	1723	5·5	3·8	2·48	1·54	0·08	1·46
TiO_2	Crystalline (rutile)	1850	80–100	80–100	2·05	1·05	0·46	2·5–2·9

*Z = formal charge (valency), a = nuclear distance.

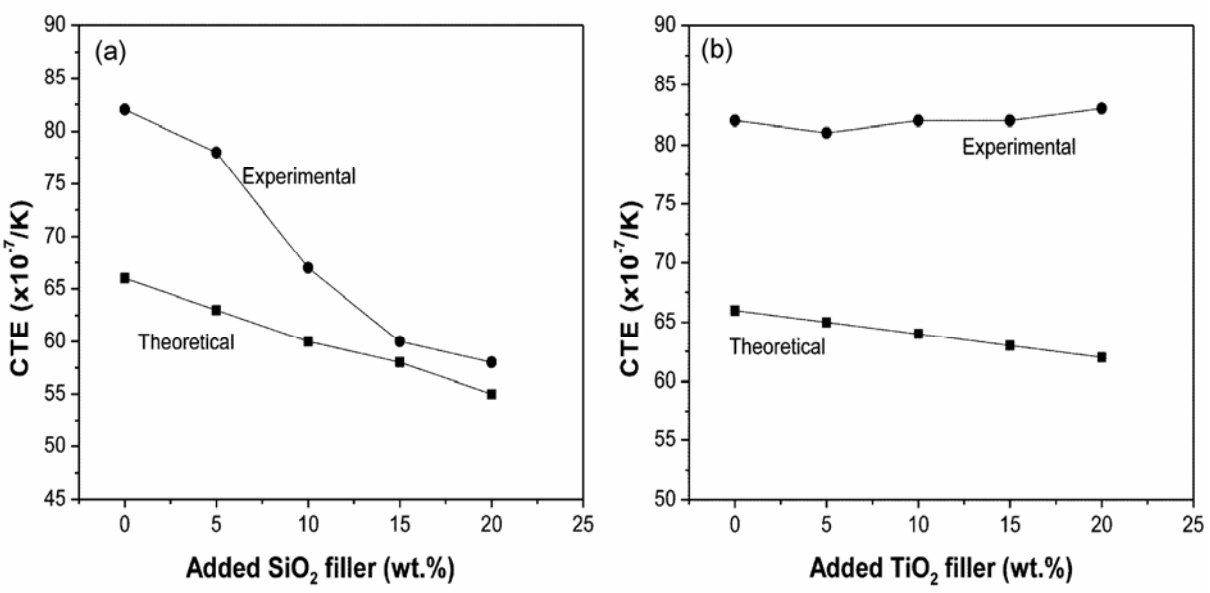

Figure 8. Comparison of variation of experimentally and theoretically predicted coefficient of thermal expansion (CTE) as a function of added (**a**) SiO_2 and (**b**) TiO_2 fillers (for composition, see table 1).

than compared to Ti–O bond strength (2·05) and Ti field strength (1·05) (Volf 1984).

3.6 *Coefficient of thermal expansion*

Comparison of variation of experimentally and theoretically predicted coefficient of thermal expansion (CTE) as a function of added SiO_2 and TiO_2 fillers is shown in figure 8. The CTE gradually decreases as SiO_2 filler content increases from 5–20 wt%. This trend correlates well with that of theoretical prediction as obtained by (1), whereas it is nearly unaffected as TiO_2 filler content increases. However, the experimental values are higher than those of theoretical predictions. In the latter case, theoretical prediction is slightly decreasing. It, thus, indicates that the change of CTE with addition of TiO_2 is not simple as formulated in (1). Similar effects have been reported by many researchers (Kim *et al* 2005, 2006; Shin *et al* 2006b) for $BaO–ZnO–B_2O_3$ and $BaO–ZnO–B_2O_3–SiO_2$ glasses on addition of SiO_2 and TiO_2 fillers. It is seen from table 4 that SiO_2 filler has very low CTE ($5·5 \times 10^{-7}$/K) as compared to the glass (82×10^{-7}/K). Therefore, the resultant CTE of the composite decreases gradually. But in case of TiO_2 filler the CTE is nearly unchanged; this is due to its very near CTE ($80–100 \times 10^{-7}$/K) as compared to glass (82×10^{-7}/K). This fact also supports the additive character of CTE of the composites with respect to their chemical components as seen earlier in the case of T_s and T_g.

The above fact can also be well understood from the bond strength values of Si–O and Ti–O bonds. The Si–O bond strength (2·48) is higher than that of Ti–O bond (2·05) (Volf 1984). The CTE in the former case decreases due to higher bond strength which results in strengthening of connectivity of the network of the resultant composites.

3.7 *Dielectric constant*

Dielectric constant (ε) of the microcomposites has been evaluated by using the following formula (Dakin 1993)

$$\varepsilon = cd/(0·0885\,A), \quad (2)$$

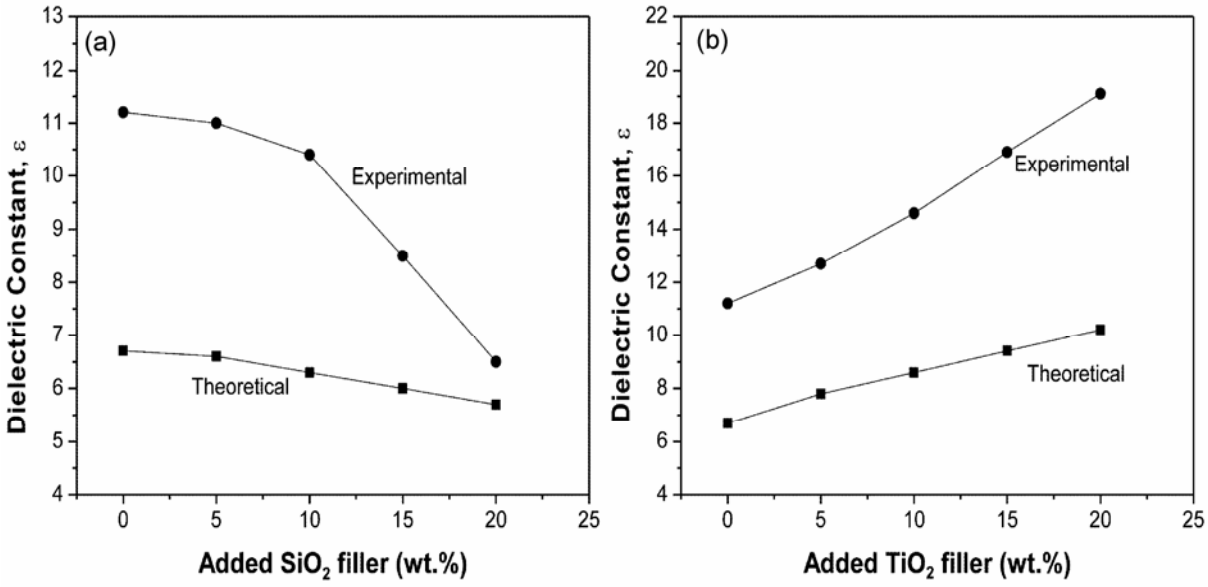

Figure 9. Comparison of variation of experimentally and theoretically predicted dielectric constant (ε) as a function of added (**a**) SiO_2 and (**b**) TiO_2 fillers at 1 MHz frequency (for composition, see table 1).

where c, d and A are capacitance in pico Farad (pF), thickness of glass or composite (cm) and area of the dielectric (cm^2) respectively.

The comparison of variation of experimentally and theoretically predicted (Kharjuzov and Zorin method (SciGlass Version 6.7)) dielectric constant as a function of added SiO_2 and TiO_2 fillers is shown in figure 9. It is seen that the dielectric constant of the composites gradually decreases with increase in SiO_2 filler content. On the other hand, dielectric constant of composites increases with the TiO_2 filler addition. All these trends correlate very well with those of theoretical predictions. However, the experimental values are higher than those of theoretical predictions. Results reported by Kim *et al* (Kim *et al* 2005, 2006; Shin *et al* 2006b) for SiO_2 and TiO_2 filler addition to $BaO–ZnO–B_2O_3$ and $BaO–ZnO–B_2O_3–SiO_2$ glasses are quite similar. It is seen from table 4 that the dielectric constant of SiO_2 filler is 3·8 which is lower than that of the glass (11·2) whereas the dielectric constant of TiO_2 filler is very high (80–100) than the glass. So the resultant dielectric constant of SiO_2 filler added composites gradually decrease whereas it increases in case of TiO_2 filler addition as expected. This is due to high polarizability (α) and refractive index (n) of TiO_2 ($\alpha = 0{\cdot}46$ and $n = 2{\cdot}5–2{\cdot}9$) than those of SiO_2 ($\alpha = 0{\cdot}08$ and $n = 1{\cdot}46$) (see table 4) (Volf 1984). Dielectric constant (ε) is related with these properties by the following Lorentz–Lorenz (3) and Maxwell (4) equations (Scholze 1991).

$$\alpha = 3M_{av}(n^2 - 1)/4(n^2 + 2)\pi N_A \rho, \quad (3)$$

$$\varepsilon = n^2, \quad (4)$$

where N_A is the Avogadro's number, and M_{av} and ρ are average molecular weight and density of the glass or composite, respectively. This once again supports in favour of the additive nature of dielectric constant like other properties such as T_s, T_g and CTE as described earlier, that is, there is a direct relationship between the property values of fillers and the resultant microcomposites. The dielectric constant is also dependent on porosity of the samples. The increase in porosity results in decrease in dielectric constant. Densities of the resulting microcomposites were found to vary from 4·2–3·3 g cm^{-3}. This is due to the combined effect of porosity (incorporated during sintering at 560°C and increased with increase in filler content) of resulting microcomposites as well as lower molecular weights of fillers (SiO_2, M.W. 60·07 and TiO_2, M.W. 79·88) compared to that of the host glass (M.W. 119·73).

4. Conclusions

In this effort to develop a lead-free eco-friendly material alternative for the white back (rear glass dielectric layer) of plasma display panels, the effect of two types of ceramic fillers (TiO_2 and SiO_2) on the softening point, glass transition temperature, coefficient of thermal expansion and dielectric properties of $ZnO–Bi_2O_3–B_2O_3$ (ZBIB) glass system has been investigated. Based on qualitative XRD, FTIR analyses and SEM images both the fillers investigated here have been found to be partially dissolved in the glass at the sintering temperature (560°C), and thus the specimen successfully formed ceramic filler particulate-reinforced glass matrix microcomposites with

a strong interfacial bonding. The SiO_2 filler has decreased the dielectric constant of the ZBIB glass (11·2), while the addition of TiO_2 has to be limited to about 10 wt% in order to ensure that the dielectric constant of the filler–glass composite is less than the currently used PbO-based glass (15). In terms of CTE, only the addition of TiO_2 filler could successfully achieve the CTE of the composite (82×10^{-7} K^{-1}) to match with the currently used PDP glass substrate such as PD 200 glass (83×10^{-7} K^{-1}). By considering all aspects of the properties, the addition of TiO_2 fillers of about 10 wt% to ZBIB glass is in general the most desirable type of filler investigated in the current work. It has yielded a softening point of 560°C, CTE of 82×10^{-7} K^{-1} and dielectric constant of 14·6, which are very close to those of the currently used PbO-based white back. The close correlation of theoretical predictions and experimental values strongly advocates the additive nature of the physical properties with respect to the chemical constituents of the composites.

Acknowledgements

This research has been supported in part by the NMITLI scheme of CSIR, New Delhi. The authors gratefully thank Dr H S Maiti, Director, CGCRI, Kolkata, for his keen interest. They also acknowledge the XRD and Ceramic Membrane Sections of this institute for carrying out the XRD and particle size measurement experiments.

References

Baia L, Stefan R, Popp J, Sinon S and Keifer W 2003 *J. Non-Cryst. Solids* **324** 109

Chang M S, Pae B J, Lee Y K, Ryu B G and Pork M H 2001 *J. Inf. Display* **2** 39

Dakin T K 1993 *Insulating materials—general properties, in standard handbook for electrical engineers* (eds) D G Fink and H W Beaty (New York: McGraw-Hill) 13th edn, pp 4–117

Fuxi G 1992 *Optical and spectroscopic properties of glass* (Berlin: Springer-Verlag)

Hiromitsu W, Hiroyuki O, Masahiko O and Kazuo H 2000 US patent 6010973

Hwang G -H, Kim W -Y, Jeon H -J and Kim Y -S 2002 *J. Am. Ceram. Soc.* **85** 2961

Kamitsos E I, Karakassides A M and Chryssikos D G 1987 *Phys. Chem. Glasses* **91** 1073

Kharlamov A A, Almeida R M and Heo J 1996 *J. Non-Cryst. Solids* **202** 233

Kim S G, Shin H, Park J S, Hong K S and Kim H 2005 *J. Electroceram.* **15** 129

Kim S -G, Park J -S, An J -S, Hong K S, Shin H and Kim H 2006 *J. Am. Ceram. Soc.* **89** 902

Kim T Y and Sunnoo J H 2000 US patent 6097151

Last J T 1957 *Phys. Rev.* **105** 1740

Lim E -S, Kim B -S, Lee J -H and Kim J -J 2006 *J. Electroceram.* **17** 359

Masahi A and Shinji K 1999 US patent 5977708

Motke S G, Yowale S P and Yawale S S 2002 *Bull. Mater. Sci.* **25** 75

Naoya H and Kazuhiro N 1999 JP patent 11246233

Priven A I 1998 *Glass Phys. & Chem.* **24** 67

Priven A I 2004 *Glass Technol.* **45** 244

Priven A I and Mazunin O V 2003 *Glass Technol.* **44** 156

Rao C N R 1963 *Chemical application of infrared spectroscopy* (New York: Academic Press)

Scholze H 1991 *Glass, nature, structure and properties* (New York: Springer) 3rd ed.

SciGlass (Glass Properties Information System), *Version 6.7*

Shin H, Kim S -G, Park J -S, An J -S, Hong K S and Kim H 2006a *J. Am. Ceram. Soc.* **89** 3258

Shin H, Kim S -G, Park J -S, Jung H S, Hong K S and Kim H 2006b *J. Mater. Res.* **21** 1753

Shinoda T, Wakitani M, Nanto T, Awaji N and Kanagu S 2000 *IEEE Trans. Electrons. Electron Dev.* **47** 77

Shiro T, Hideaki M, Tadahiko U and Koji K 1998 JP patent 10338547

Song J -Y and Choi S -Y 2006 *Display* **27** 112

Song J -Y, Park T -J and Choi S -Y 2006 *J. Non-Cryst. Solids* **352** 5403

Uma T and Nogami M 2007 *J. Phys. Chem.* **C111** 16635

Vernacotola D E 1994 *Key Engg. Mater.* **94–95** 379

Vernacotola D E and Shelby J E 1993 *Ceram. Trans.* **29** 215

Volf M B 1984 *Chemical approach to glass* (Amsterdam: Elsevier)